HAL
open science

Interplay between spontaneous decay rates and Lamb shifts in open photonic systems

Emmanuel Lassalle, Nicolas Bonod, Thomas Durt, Brian Stout

To cite this version:

Emmanuel Lassalle, Nicolas Bonod, Thomas Durt, Brian Stout. Interplay between spontaneous decay rates and Lamb shifts in open photonic systems. Optics Letters, 2018, 43 (9), 10.1364/OL.43.001950 . hal-01774673

HAL Id: hal-01774673

https://hal.science/hal-01774673v1

Submitted on 23 Apr 2018

HAL is a multi-disciplinary open access archive for the deposit and dissemination of scientific research documents, whether they are published or not. The documents may come from teaching and research institutions in France or abroad, or from public or private research centers.

L'archive ouverte pluridisciplinaire **HAL**, est destinée au dépôt et à la diffusion de documents scientifiques de niveau recherche, publiés ou non, émanant des établissements d'enseignement et de recherche français ou étrangers, des laboratoires publics ou privés.

Interplay between spontaneous decay rates and Lamb shifts in open photonic systems

Emmanuel Lassalle,* Nicolas Bonod, Thomas Durt, and Brian Stout†
Aix Marseille Univ, CNRS, Centrale Marseille, Institut Fresnel, Marseille, France
(Dated: April 23, 2018)

In this letter, we describe the modified decay rate and photonic Lamb (frequency) shift of quantum emitters in terms of the resonant states of a neighboring photonic resonator. This description illustrates a fundamental distinction in the behaviors of closed (conservative) and open (dissipative) systems: the Lamb shift is bounded by the emission linewidth in closed systems while it overcomes this limit in open systems.

I. INTRODUCTION

The coupling between quantum emitters (QE) and resonant photonic nanostructures is at the heart of nanophotonics [1]. The resonances of a given structure characterize its optical response to an excitation electromagnetic (EM) field, and can be of different nature: Mie resonances in dielectric structures [2], or surface plasmons in metallic ones [3]. A powerful tool to describe both types of resonances is the use of resonant states, also called quasi-normal modes (QNMs), which are the natural modes of the photonic system. A remarkable advantage of this framework is that it allows to generalize the usual cavity-quantum electrodynamics (cQED) figures of merit characterizing the interaction between a dipole source and the resonance of a cavity, such as the quality factor Q or mode volume V, to the case of open and/or absorbing systems (and also taking into account material dispersion) that are almost always found in nanophotonics [4–6]. For instance, the use of QNMs has been proposed to express the spontaneous decay rate of a QE coupled to an open photonic resonator in [5, 6].

In this work, we express the photonic Lamb shift (*i.e.* the shift of the emission frequency due to the neighboring environment) in terms of the QNMs. We start from the general quantum optics results, valid in the weak-coupling regime, that relate the spontaneous decay rate and photonic Lamb shift of a two-level QE to the Green tensor. We then make use of the resonant states of the photonic system to which the QE couples to expand the Green tensor and derive analytic expressions for the decay rate and Lamb shift involving the following figures of merit: quality factor, mode volume and Purcell factor. The derived expressions reveal an interplay between the decay rate and the Lamb shift, and in the single-resonance limit, we show that: (i) for conservative (Hermitian) systems, *i.e.* closed and non-absorbing, or for systems with small losses characterized by high quality factors, the Lamb shift always lies within the emission linewidth (equal to the decay rate), whereas (ii) for dissipative, *i.e.* open and/or absorbing, systems (non-Hermitian), the Lamb shift can go beyond this fundamental limit (see [7] with references therein and [8]).

* emmanuel.lassalle@fresnel.fr
† brian.stout@fresnel.fr

II. LAMB SHIFT AND DECAY RATE INTERPLAY

In the presence of a neighboring photonic structure, a two-level QE will experience a new decay rate γ^* and emission frequency ω^* compared to the case of free-space denoted by γ_0 and ω_0, respectively. Using the macroscopic quantum optics results for a two-level atom coupled to a general dispersive and absorbing medium, one can write the environment-modified decay rate γ^* and photonic Lamb shift $\Delta\omega$ defined by $\Delta\omega \equiv \omega^* - \omega_0$ in terms of the Green tensor $\overleftrightarrow{\mathbf{G}}$ (defined in Appendix VI A) that fully contains all the properties of the EM environment of the emitter (we assume a constant relative permeability $\mu = 1$) [9, 10]

$$\frac{\gamma^*}{\gamma_0} = 1 + \frac{6\pi c}{\omega_0} \times \mathbf{u}_p \cdot \mathrm{Im}(\overleftrightarrow{\mathbf{G}}_s(\mathbf{r}_0, \mathbf{r}_0, \omega_0)) \cdot \mathbf{u}_p \ , \quad (1)$$

$$\frac{\Delta\omega}{\gamma_0} = -\frac{3\pi c}{\omega_0} \times \mathbf{u}_p \cdot \mathrm{Re}(\overleftrightarrow{\mathbf{G}}_s(\mathbf{r}_0, \mathbf{r}_0, \omega_0)) \cdot \mathbf{u}_p \ , \quad (2)$$

where c is the speed of light in vacuum, $\mathbf{r}_0$ the atom position and $\mathbf{u}_p$ the unit vector in the direction of its electric dipole moment: $\mathbf{p}_0 = p_0\mathbf{u}_p$. Note that in these expressions, the total Green tensor $\overleftrightarrow{\mathbf{G}}$ has been decomposed into the "free-space" part $\overleftrightarrow{\mathbf{G}}_0$ (*i.e.* the Green tensor in the absence of the neighboring structure) and a "scattered" part $\overleftrightarrow{\mathbf{G}}_s$ (which defines the contribution of the photonic system) as: $\overleftrightarrow{\mathbf{G}} = \overleftrightarrow{\mathbf{G}}_0 + \overleftrightarrow{\mathbf{G}}_s$, and the quantities have been normalized by the free-space decay rate $\gamma_0 = 2\omega_0^2/(\epsilon_0\hbar c^2)|\mathbf{p}_0|^2\mathbf{u}_p \cdot \mathrm{Im}(\overleftrightarrow{\mathbf{G}}_0(\mathbf{r}_0, \mathbf{r}_0, \omega_0)) \cdot \mathbf{u}_p$ where $\mathbf{u}_p \cdot \mathrm{Im}(\overleftrightarrow{\mathbf{G}}_0(\mathbf{r}_0, \mathbf{r}_0, \omega_0)) \cdot \mathbf{u}_p = \omega_0/6\pi c$. Moreover, as far as the Lamb shift is concerned, the integral part over all frequencies (see [10]) has been omitted. Eqs. (1) and (2) obtained within a two-level system model are the same as the ones of the decay rate and radiative frequency-shift of a classical electric dipole normalized by the classical decay rate in free space [11]. A more complete treatment of the Lamb shift for real multilevel atoms can be found in [12].

We assume that the scattered part of the Green tensor $\overleftrightarrow{\mathbf{G}}_s$ can be expanded in terms of the resonant states of the photonic system, and we use the spectral representation

of the Green tensor [6, 13, 14]

$$\overleftrightarrow{\mathbf{G}}_s(\mathbf{r},\mathbf{r}',\omega) \simeq c^2 \sum_\alpha \frac{\mathbf{E}_\alpha(\mathbf{r}) \otimes \mathbf{E}_\alpha(\mathbf{r}')}{2\omega(\omega_\alpha - \omega)} \tag{3}$$

where $\mathbf{E}_\alpha$ are the QNM fields normalized according to Muljarov *et al.* [6, 14], $\omega_\alpha \equiv \omega'_\alpha + \mathrm{i}\,\omega''_\alpha$ are the QNM complex frequencies and $\otimes$ denotes the tensor product (definitions in Appendix VI B). When plugging Eq. (3) in Eqs. (1) and (2), one immediately gets

$$\frac{\gamma^*}{\gamma_0} = 1 + \frac{3\pi\, c^3}{\omega_0^2} \sum_\alpha \mathrm{Im}\left(\frac{1}{V_\alpha(\omega_\alpha - \omega_0)}\right) \tag{4}$$

$$\frac{\Delta\omega}{\gamma_0} = -\frac{3\pi\, c^3}{2\omega_0^2} \sum_\alpha \mathrm{Re}\left(\frac{1}{V_\alpha(\omega_\alpha - \omega_0)}\right) \tag{5}$$

where V_α is the mode volume of the QNM α defined as

$$V_\alpha \equiv \frac{1}{(\mathbf{u_p} \cdot \mathbf{E}_\alpha(\mathbf{r}_0))^2} \tag{6}$$

in which the QNM field $\mathbf{E}_\alpha$ is taken at the QE position $\mathbf{r}_0$. This figure of merit characterizes the coupling between the QE and the resonance α through the real part (the larger $\mathrm{Re}(1/V_\alpha)$, the better is the coupling) [15], and also energy dissipations through the presence of an imaginary part (a large $\mathrm{Im}(1/V_\alpha)$ indicates important energy dissipations) [5]. We next introduce the Purcell factor F_α, which corresponds to the enhancement of the total decay rate γ^* in comparison to γ_0 due the the resonance α and for a perfect spectral match ($\omega_0 = \omega'_\alpha$),

$$F_\alpha \equiv \frac{6\pi\, c^3}{\omega_\alpha'^3} Q_\alpha \mathrm{Re}\,(1/V_\alpha)\ , \tag{7}$$

with the usual quality factor Q_α defined as $Q_\alpha \equiv -\omega'_\alpha/(2\omega''_\alpha)$ ($\omega''_\alpha < 0$ due to the convention used for the Fourier transform "$e^{-\mathrm{i}\omega t}$"). Expressions (4) and (5) can then be recast in a form revealing an interplay between Lamb shift and decay rate (see derivation in Appendix VI C)

$$\frac{\gamma^*}{\gamma_0} = 1 + \sum_\alpha \left\{ \frac{\gamma_\alpha^H}{\gamma_0} - 2\frac{\Delta\omega_\alpha^H}{\gamma_0} \frac{\mathrm{Im}(1/V_\alpha)}{\mathrm{Re}(1/V_\alpha)} \right\} \tag{8}$$

$$\frac{\Delta\omega}{\gamma_0} = \sum_\alpha \left\{ \frac{\Delta\omega_\alpha^H}{\gamma_0} + \frac{1}{2}\frac{\gamma_\alpha^H}{\gamma_0} \frac{\mathrm{Im}(1/V_\alpha)}{\mathrm{Re}(1/V_\alpha)} \right\} \tag{9}$$

where the expressions of γ_α^H/γ_0 and $\Delta\omega_\alpha^H/\gamma_0$ are

$$\frac{\gamma_\alpha^H}{\gamma_0} = F_\alpha \left(\frac{\omega'_\alpha}{\omega_0}\right)^2 \frac{\omega''^2_\alpha}{(\omega'_\alpha - \omega_0)^2 + \omega''^2_\alpha} \tag{10}$$

$$\frac{\Delta\omega_\alpha^H}{\gamma_0} = F_\alpha \left(\frac{\omega'_\alpha}{\omega_0}\right)^2 \frac{\omega''_\alpha}{2} \frac{\omega'_\alpha - \omega_0}{(\omega'_\alpha - \omega_0)^2 + \omega''^2_\alpha}\ . \tag{11}$$

The superscript H indicates "Hermitian", because for conservative systems, and more realistically for systems with small losses, $\mathrm{Im}(V_\alpha) \simeq 0$ and one recovers the sum of Lorentzians which is phenomenologically used for high-Q cavities [5]: $\gamma^*/\gamma_0 = 1 + \sum_\alpha \gamma_\alpha^H/\gamma_0$. In contrast, for dissipative systems characterized by $\mathrm{Im}(V_\alpha) \neq 0$ [5], Eqs. (8) and (9) reveal an interplay between the "Hermitian" decay rates γ_α^H and Lamb shifts $\Delta\omega_\alpha^H$. This constitutes our first result.

III. EXAMPLE

As an example, let us apply Eqs. (8) and (9) to two situations of a QE coupled to an open photonic system: (i) dielectric silicon (Si) nanosphere with no absorption (and no dispersion) and (ii) plasmonic silver (Ag) nanosphere with absorption (and dispersion) (see insets in Fig. 1 (a-c)). For spherical resonators, the QNM fields are the multipolar fields, labeled by four numbers $\{q, n, m, l\}$ where q labels a magnetic ($q = 1$) or an electric ($q = 2$) mode, $n = 1, 2, ..., \infty$ is the multipolar order, $m = -n, ..., n$ is the orbital (or azimutal) number, and l numerates the different QNM complex frequencies $\omega_{q,n,m,l}$ found for a fixed combination of $\{q, n, m\}$, which are the poles of the Mie coefficients [8, 15, 16]. Therefore, for spherical resonators the sums over α in Eqs. (8) and (9) become: $\sum_\alpha \to \sum_{q,n,m,l}$. Moreover, for a given set of $\{q, n, l\}$, the QNMs with a different number m are degenerate (*i.e.* have the same complex frequency $\omega_{q,n,m,l}$), and the sum can be recast in the form $\sum_{q,n,l}$ with "effective" mode volumes defined as $1/V_{q,n,l} \equiv \sum_m 1/V_{q,n,m,l}$ (see Appendix E in [6] and also [8]).

In the following, the mode volumes given by Eq. (6), and appearing in the QNM formulas Eqs. (8) and (9), are computed using the analytical expressions of the QNM fields $\mathbf{E}_\alpha$ derived for a spherical resonator shape in [14] for non-dispersive materials (*i.e.* with a constant permittivity) and in [6] for dispersive materials (*i.e.* with a permittivity that depends on the frequency ω). The QNM complex frequencies are found by solving a transcendental equation (giving the poles of the Mie coefficients) with the FindRoot function of Mathematica, and where we use an analytic continuation of the permittivity in the complex plane in the case of dispersive materials.

For the calculations, we consider an electric dipole emitter radially oriented (and therefore only coupled to the electric modes $q = 2$ [17]) and located at a distance $d = 10\,\mathrm{nm}$ from the sphere. The Si nanosphere (dielec-

	$\alpha = (n, l)$	λ_α (nm)	V_α (nm^3)
Si	$(2, 1)$	$547.3 + \mathrm{i}4.7$	$(17.573 - \mathrm{i}6.974) \cdot 10^6$
	$(2, 2)$	$329.7 + \mathrm{i}106.3$	$(1.222 + \mathrm{i}1.063) \cdot 10^6$
Ag	$(1, 1)$	$375.6 + \mathrm{i}15.5$	$(0.525 - \mathrm{i}0.023) \cdot 10^6$

TABLE I. QNMs complex wavelengths λ_α and mode volumes V_α appearing in Eqs. (8) and (9) and used to obtain the results of Fig. 1.

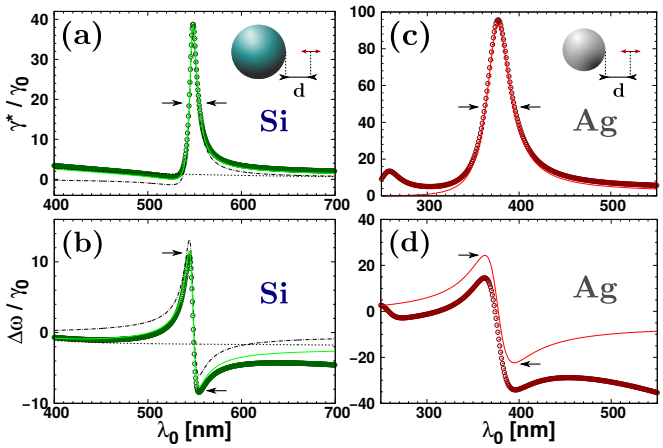

FIG. 1. Comparison between QNM calculations using Eqs. (8) and (9) (lines) and exact calculations using Mie theory (circles) of the decay rate γ^* and Lamb shift $\Delta\omega$ (normalized by γ_0) as a function of the emitter transition wavelength $\lambda_0 = 2\pi c/\omega_0$, for two configurations: (a-b) silicon (Si) and (c-d) silver (Ag) nanospheres of radii $a = 120\,\text{nm}$ and $a = 20\,\text{nm}$, respectively. In all cases, the emitter (red arrow) is radially oriented and located at a distance $d = 10\,\text{nm}$ from the sphere. For Si [Ag], only the electric quadrupolar [dipolar] contribution to the decay rate (a) [(c)] and Lamb shift (b) [(d)] is shown.

tric permittivity $\varepsilon = 16$) has a radius of $a = 120\,\text{nm}$, exhibiting a dominant electric quadrupolar resonance at 547 nm, and the Ag nanosphere (Drude-Lorentz model for the dielectric permittivity taken from [18]) has a radius of $a = 20\,\text{nm}$, exhibiting a dominant electric dipolar resonance at 375 nm. For the Si configuration, we show in Figs. 1 (a-b) the electric quadrupolar contribution ($n = 2$) to the decay rate γ^* and Lamb shift $\Delta\omega$ as a function of the emitter transition wavelength $\lambda_0 = 2\pi c/\omega_0$, calculated from the QNM formulas (8) and (9) (solid green line), and compared with the exact Mie theory (green dots). We find several QNMs associated with this quadrupolar resonance, and by using the two dominant QNMs (whose mode volumes and complex wavelengths defined as $\lambda_\alpha \equiv 2\pi c/\omega_\alpha$ are given in Table I), the QNM formulas work very well, with a better result for the decay rate than for the Lamb shift for which one can see a certain discrepancy at high wavelengths. The two individual contributions of the QNMs used in the expansion are also shown (dashed black lines in (a-b)).

For the Ag configuration we show in Figs. 1 (c-d) the dominant dipolar contribution ($n = 1$) to the decay rate γ^* and Lamb shift $\Delta\omega$ as a function of the emitter transition wavelength λ_0, calculated from Eqs. (8) and (9) (solid red lines) and compared with the Mie theory (red dots). We only find a single QNM associated with this dipolar resonance (whose mode volume and complex wavelength are given in Table I). The agreements are quite good for the decay rate, but one can see certain discrepancies for the Lamb shift (the resonance around 250 nm is a spurious resonance peculiar to the model of permittivity used [19]). These Lamb shift discrepancies (more important in the metallic case) appear to be related to omitted non-resonant contributions (see Eq. (4) in [20] and Eq. (16) in [21]), which impact more the Lamb shift than the decay rate in the near field. Finally, let us emphasize the presence of an imaginary part in the mode volumes displayed in Table I. In the dielectric case, the imaginary part characterizes the radiative losses and in the plasmonic case, it characterizes both radiative and absorption losses.

IV. MAXIMUM LAMB SHIFTS IN THE SINGLE-RESONANCE APPROXIMATION

From here on, we work under the assumption that the QE couples to a single resonance α. First, we revisit the case of conservative or low-loss systems for which $\text{Im}(V_\alpha) \simeq 0$. In this case, Eqs. (8) and (9) become $\gamma^*/\gamma_0 = 1 + \gamma_\alpha^H/\gamma_0$ and $\Delta\omega/\gamma_0 = \Delta\omega_\alpha^H/\gamma_0$, and we can see that the decay rate γ_α^H and the Lamb shift $\Delta\omega_\alpha^H$ are dissociated and there is no interplay. We want to assess the maximum frequency shift $\Delta\omega_{\max}$, that occurs when the QE natural frequency ω_0 is detuned by $\pm\omega_\alpha''$ compared to the QNM resonance frequency ω_α'. At these particular frequencies $\omega_0 = \omega_\alpha' \mp \omega_\alpha''$, the decay rate and Lamb shift (pointed out with arrows in Fig. 1) are (see Appendix VI D)

$$\frac{\gamma^*}{\gamma_0} = 1 + \frac{1}{2}F_\alpha + O(Q_\alpha^{-1}) \tag{12}$$

$$\frac{\Delta\omega_{\max}}{\gamma_0} = \pm\frac{1}{4}F_\alpha + O(Q_\alpha^{-1}) \tag{13}$$

($\Delta\omega_{\max} \simeq +1/4F_\alpha$ when $\omega_0 = \omega_\alpha' - \omega_\alpha''$ and $\Delta\omega_{\max} \simeq -1/4F_\alpha$ when $\omega_0 = \omega_\alpha' + \omega_\alpha''$). We retrieve in this ideal case the expressions for the maximum frequency shift that were derived in [22], Eq. (35), where they considered a two-level atom inside a cavity whose resonance was phenomenologically described by a Lorentzian. For large decay rate enhancements $\gamma^* \gg \gamma_0$, the first term in the right hand side of Eq. (12) can be omitted and we finally end up with the following relations for the maximum photonic Lamb shift

$$\Delta\omega_{\max} = \pm\frac{\gamma^*}{2}\,. \tag{14}$$

Before commenting this result, let us first recall that in the weak-coupling regime, the emitted-light spectrum of the QE has a Lorentzian line shape [9], and one usually takes the full width at half maximum (FWHM) $\hbar\gamma^*$ as a measure of the energy spread δE, called energy level width or emission linewidth. This leads to the relation between the energy level width and the lifetime of the excited state (defined as $\tau \equiv 1/\gamma^*$): $\delta E\,\tau = \hbar$, which can be seen as a time-energy uncertainty relation (see *e.g.* [23]). Thus — and this is our second result — for conservative systems, or systems with weak energy dissipations, and in

the single-resonance approximation, Eq. (14) shows that the photonic Lamb shift always lies within the emission linewidth. As already pointed out in [22], this makes it difficult to observe as a shift of the spectral line.

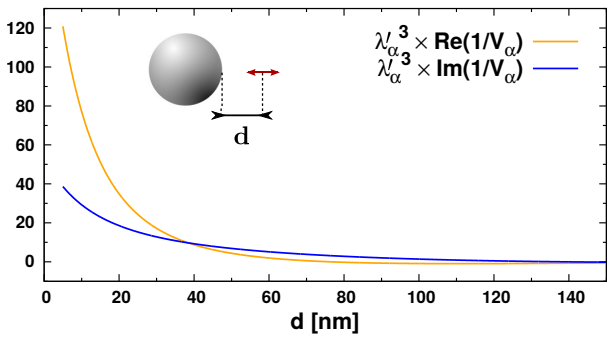

FIG. 2. Inverse of the mode volume $1/V_\alpha$ of the dipolar QNM of a silver nanosphere (radius $a = 50\,\mathrm{nm}$), as a function of the distance d (real part in orange and imaginary part in blue), for an emitter radially oriented (red arrow). Note that $1/V_\alpha$ has been multiplied by the cube of the QNM resonance wavelength $\lambda'_\alpha = 411.6\,\mathrm{nm}$.

Let us now turn to the case of dissipative systems, for which $\mathrm{Im}(V_\alpha) \neq 0$. In this case, the decay rate and Lamb shift are described by Eqs. (8) and (9), respectively. At the frequencies $\omega_0 = \omega'_\alpha \mp \omega''_\alpha$, these expressions reduce to (see Appendix VI D)

$$\frac{\gamma^*}{\gamma_0} = 1 + \frac{1}{2}F_\alpha\left[1 \mp \frac{\mathrm{Im}(1/V_\alpha)}{\mathrm{Re}(1/V_\alpha)}\right] + O(Q_\alpha^{-1}) \qquad (15)$$

$$\frac{\Delta\omega_{\max}}{\gamma_0} = \pm\frac{1}{4}F_\alpha\left[1 \pm \frac{\mathrm{Im}(1/V_\alpha)}{\mathrm{Re}(1/V_\alpha)}\right] + O(Q_\alpha^{-1}) \qquad (16)$$

(when $\omega_0 = \omega'_\alpha - \omega''_\alpha$ one must take the upper sign and when $\omega_0 = \omega'_\alpha + \omega''_\alpha$ one must take the lower sign). For large decay rate enhancements $\gamma^* \gg \gamma_0$, the first term in the right hand side of (15) can be neglected and we get the following relation between the maximum Lamb shift and decay rate

$$\Delta\omega_{\max} = \pm\frac{[\mathrm{Re}(1/V_\alpha) \pm \mathrm{Im}(1/V_\alpha)]}{[\mathrm{Re}(1/V_\alpha) \mp \mathrm{Im}(1/V_\alpha)]}\frac{\gamma^*}{2}\,. \qquad (17)$$

In sharp contrast with Eq. (14) valid for conservative or high-Q systems, Eq. (17) shows that for dissipative systems, the Lamb shift is not bounded by the emission linewidth, and can go beyond this limit. This is our third result.

To illustrate this fundamental distinction in the behavior of conservative and dissipative systems, we consider in the following a QE radially oriented and coupled to the plasmonic dipolar resonance of a silver nanoparticle of radius $a = 50\,\mathrm{nm}$ (see inset in Fig. 2). The complex wavelength $\lambda_\alpha = \lambda'_\alpha + \mathrm{i}\lambda''_\alpha$ of the dipolar QNM is calculated to be $\lambda_\alpha = 411.6 + \mathrm{i}50.8$ nm, which gives a quality factor $Q_\alpha = \lambda'_\alpha/(2\lambda''_\alpha) = 4$. The QE transition wavelength $\lambda_0 = 2\pi c/\omega_0$ is assumed to be $\lambda_0 = 372$ nm. This corresponds to the case $\omega_0 = \omega'_\alpha - \omega''_\alpha$ for which the Lamb shift $\Delta\omega_{\max}$ is maximum and positive and given by Eq. (16) (taking the positive sign), and the decay rate γ^* is the one given by Eq. (15) (taking the negative sign). First, we plot in Fig. 2 (the inverse of) the mode volume V_α of the dipolar QNM as a function of the distance d between the QE and the nanoparticle. One can see that $\mathrm{Re}(1/V_\alpha)$, which characterizes the coupling between the QE and the nanoparticle, increases as d decreases (orange curve), which is in accordance with the expectation that the coupling increases as the QE gets closer to the resonator. Moreover, one can see the presence of energy dissipations through a non-negligible $\mathrm{Im}(1/V_\alpha)$ (blue curve), which is expected when considering the low quality factor of the resonance $Q_\alpha = 4$.

Accordingly, the decay rate γ^* [Eq. (15)] and maximum Lamb shift $\Delta\omega_{\max}$ [Eq. (16)] will increase as d decreases in a similar way as $\mathrm{Re}(1/V_\alpha)$ in Fig. 2 (because the Purcell factor appearing in their expression is $F_\alpha \propto \mathrm{Re}(1/V_\alpha)$ [see Eq. (7)]). More importantly, dissipations, through the presence of $\mathrm{Im}(1/V_\alpha)$ in Eqs. (15) and (16), will weaken the decay rate (due to the negative sign in Eq. (15)) and increase the Lamb shift (due to the positive sign in Eq. (16)), compared to the conservative case where $\mathrm{Im}(1/V_\alpha) = 0$. To see this effect, we plot in Fig. 3 the ratio $\Delta\omega_{\max}/\gamma^*$ as a function of the distance d, for the dissipative case (blue curve) and the ideal conservative case (orange curve). The limit $\Delta\omega = \gamma^*/2$ is also shown (dashed black line). One can see that contrary to the conservative case where the Lamb shift is bounded by $\gamma^*/2$, dissipations allow to fulfill the condition $\Delta\omega > \gamma^*/2$. We compare this result with the Mie calculations taking into account only the electric dipolar ($n = 1$) response of the nanoparticle (red curve). Despite a decrease of the magnitude (that might be explained by the non-resonant contributions discussed previously), the Mie calculations still show a Lamb shift that overcomes the limit of conservative systems under a dipolar approximation.

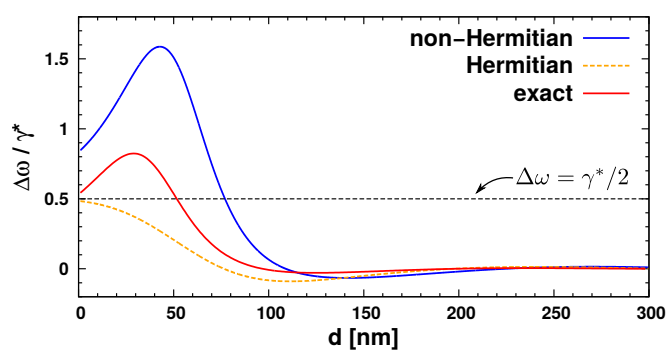

FIG. 3. Ratio between the Lamb shift $\Delta\omega_{\max}$ and the decay rate $\gamma*$ as a function of the distance d, calculated from Eqs. (15) and (16) (in blue), from Eqs. (12) and (13) (in orange), and from the Mie theory (in red), for the same configuration as in Fig. 2. A guide-to-the-eye shows the limit $\Delta\omega = \gamma^*/2$.

V. CONCLUSION

To sum up, using a quasi-normal mode description, we derive general expressions for the environment-modified decay rate and photonic Lamb shift, valid for open (dissipative) resonators. In the single-resonance approximation, we consider the maximum level shift that can be expected, and we show a remarkable difference between closed (conservative) and open (dissipative) systems: while for conservative systems, the Lamb shift remains within the emission linewidth, it can go beyond this fundamental range for dissipative systems.

VI. APPENDIX

A. Definition of the Green tensor

The Green tensor $\overleftrightarrow{\mathbf{G}}(\mathbf{r},\mathbf{r}',\omega)$ is defined as the solution of the classical Maxwell's equations with a δ function source term

$$\nabla\times\nabla\times\overleftrightarrow{\mathbf{G}}-\frac{\omega^2}{c^2}\varepsilon\overleftrightarrow{\mathbf{G}}=\overleftrightarrow{\mathbf{I}}\,\delta(\mathbf{r}-\mathbf{r}') \tag{18}$$

with the proper boundary conditions. $\overleftrightarrow{\mathbf{I}}$ is the unit tensor and $\varepsilon(\mathbf{r},\omega)$ is the relative permittivity. Note that we assume a constant relative permeability $\mu=1$. The Green tensor defined by this equation has the units: $[\overleftrightarrow{\mathbf{G}}]=\mathrm{m}^{-1}$.

B. Definition of the resonant states

The resonant states $\mathbf{E}_\alpha(\mathbf{r})$ of the photonic system are defined as the solutions of the Maxwell's equations in the absence of source

$$\nabla\times\nabla\times\mathbf{E}_\alpha=\frac{\omega_\alpha^2}{c^2}\varepsilon(\mathbf{r},\omega)\mathbf{E}_\alpha \tag{B1}$$

where ε is the relative permittivity of the resonator and where a constant relative permeability $\mu=1$. Moreover, these eigenmodes satisfy outgoing wave boundary conditions [4, 5, 14]. Because of the boundary conditions, the eigenfrequencies ω_α associated to the eigenmodes $\mathbf{E}_\alpha$ are complex: $\omega_\alpha=\omega'_\alpha+\mathrm{i}\,\omega''_\alpha$, where $\omega''_\alpha<0$ due to the convention used for the Fourier transform "$e^{-\mathrm{i}\omega t}$". In this letter, we follow the normalization condition of Doost *et al.* [6, 14] where the resonant modes are normalized according to

$$1=\frac{1}{2}\int_V\mathbf{E}_\alpha\cdot\left[\frac{\partial(\omega\varepsilon)}{\partial(\omega)}+\varepsilon\right]\mathbf{E}_\alpha\,\mathrm{d}\mathbf{r}+\frac{c^2}{2\omega_\alpha^2}\oint_{\partial V}\left[\mathbf{E}_\alpha\cdot\frac{\partial}{\partial s}(\mathbf{r}\cdot\nabla)\mathbf{E}_\alpha-(\mathbf{r}\cdot\nabla)\mathbf{E}_\alpha\cdot\frac{\partial\mathbf{E}_\alpha}{\partial s}\right]\mathrm{d}S\,. \tag{B2}$$

All the quantities that depend on ω are taken at $\omega=\omega_\alpha$. The first integral is taken over a volume V enclosing the photonic system, and the second integral is taken over a closed surface ∂V of the volume V, with the normal derivative $\partial/\partial s=\mathbf{n}\cdot\nabla$, $\mathbf{n}$ being the outward unit vector normal to the surface. This normalization sets the unity of the electric fields as: $[\mathbf{E}_\alpha]=\mathrm{m}^{-3/2}$.

C. Derivation of Eqs. (8), (9), (10) and (11)

Here we derive the interplay relations between the decay rate and Lamb shift (8), (9), (10) and (11). For Hermitian systems, $\mathrm{Im}(1/V_\alpha)=0$. In this case, Eqs. (4) and (5) (main text) can be written as

$$\frac{\gamma^*}{\gamma_0}=1+\frac{3\pi\,c^3}{\omega_0^2}\sum_\alpha\mathrm{Re}\left(\frac{1}{V_\alpha}\right)\mathrm{Im}\left(\frac{1}{\omega_\alpha-\omega_0}\right) \tag{B3}$$

$$\frac{\Delta\omega}{\gamma_0}=-\frac{3\pi\,c^3}{2\omega_0^2}\sum_\alpha\mathrm{Re}\left(\frac{1}{V_\alpha}\right)\mathrm{Re}\left(\frac{1}{\omega_\alpha-\omega_0}\right)\,. \tag{B4}$$

We then define the Hermitian decay rate and Lamb shift associated to the resonance α as

$$\frac{\gamma_\alpha^H}{\gamma_0}\equiv\frac{3\pi\,c^3}{\omega_0^2}\mathrm{Re}\left(\frac{1}{V_\alpha}\right)\mathrm{Im}\left(\frac{1}{\omega_\alpha-\omega_0}\right) \tag{B5}$$

$$\frac{\Delta\omega_\alpha^H}{\gamma_0}\equiv-\frac{3\pi\,c^3}{2\omega_0^2}\mathrm{Re}\left(\frac{1}{V_\alpha}\right)\mathrm{Re}\left(\frac{1}{\omega_\alpha-\omega_0}\right)\,, \tag{B6}$$

so that the total decay rate and Lamb shift read $\gamma^*=\gamma_0+\sum_\alpha\gamma_\alpha^H$ and $\Delta\omega=\sum_\alpha\Delta\omega_\alpha^H$ respectively.

For non-Hermitian systems, $\mathrm{Im}(1/V_\alpha)\neq 0$. In this case, Eqs. (4) and (5) present an extra term compared to the Hermitian case

$$\frac{\gamma^*}{\gamma_0}=1+\frac{3\pi\,c^3}{\omega_0^2}\sum_\alpha\mathrm{Re}\left(\frac{1}{V_\alpha}\right)\mathrm{Im}\left(\frac{1}{\omega_\alpha-\omega_0}\right)+\frac{3\pi\,c^3}{\omega_0^2}\sum_\alpha\mathrm{Im}\left(\frac{1}{V_\alpha}\right)\mathrm{Re}\left(\frac{1}{\omega_\alpha-\omega_0}\right) \tag{B7}$$

$$\frac{\Delta\omega}{\gamma_0}=-\frac{3\pi\,c^3}{2\omega_0^2}\sum_\alpha\mathrm{Re}\left(\frac{1}{V_\alpha}\right)\mathrm{Re}\left(\frac{1}{\omega_\alpha-\omega_0}\right)+\frac{3\pi\,c^3}{2\omega_0^2}\sum_\alpha\mathrm{Im}\left(\frac{1}{V_\alpha}\right)\mathrm{Im}\left(\frac{1}{\omega_\alpha-\omega_0}\right)\,. \tag{B8}$$

By making use of (B5) and (B6), these expressions can be recast in the form

$$\frac{\gamma^*}{\gamma_0}=1+\sum_\alpha\left\{\frac{\gamma_\alpha^H}{\gamma_0}-2\frac{\Delta\omega_\alpha^H}{\gamma_0}\frac{\mathrm{Im}(1/V_\alpha)}{\mathrm{Re}(1/V_\alpha)}\right\} \tag{B9}$$

$$\frac{\Delta\omega}{\gamma_0}=\sum_\alpha\left\{\frac{\Delta\omega_\alpha^H}{\gamma_0}+\frac{1}{2}\frac{\gamma_\alpha^H}{\gamma_0}\frac{\mathrm{Im}(1/V_\alpha)}{\mathrm{Re}(1/V_\alpha)}\right\} \tag{B10}$$

which are the expressions (8) and (9) of the main text.

Now, we show how the expressions (B5) and (B6) for γ_α^H and $\Delta\omega_\alpha^H$ respectively can be rewritten in the form of Eqs. (10) and (11) (main text). First, by multiplying by the complex conjugate, we can explicitely write (we remind that we defined $\omega_\alpha \equiv \omega'_\alpha + \mathrm{i}\,\omega''_\alpha$)

$$\mathrm{Re}\left(\frac{1}{\omega_\alpha - \omega_0}\right) = \frac{\omega'_\alpha - \omega_0}{|\omega_\alpha - \omega_0|^2} = \frac{\omega'_\alpha - \omega_0}{(\omega'_\alpha - \omega_0)^2 + \omega''^2_\alpha} \tag{B11}$$

$$\mathrm{Im}\left(\frac{1}{\omega_\alpha - \omega_0}\right) = \frac{-\omega''_\alpha}{|\omega_\alpha - \omega_0|^2} = \frac{-\omega''_\alpha}{(\omega'_\alpha - \omega_0)^2 + \omega''^2_\alpha} \tag{B12}$$

By reporting these expressions into Eqs. (B5) and (B6), we get

$$\frac{\gamma_\alpha^H}{\gamma_0} = \frac{3\pi\, c^3}{\omega_0^2}\,\mathrm{Re}\left(\frac{1}{V_\alpha}\right)\frac{-\omega''_\alpha}{(\omega'_\alpha - \omega_0)^2 + \omega''^2_\alpha} \tag{B13}$$

$$\frac{\Delta\omega_\alpha^H}{\gamma_0} = -\frac{3\pi\, c^3}{2\omega_0^2}\,\mathrm{Re}\left(\frac{1}{V_\alpha}\right)\frac{\omega'_\alpha - \omega_0}{(\omega'_\alpha - \omega_0)^2 + \omega''^2_\alpha} \tag{B14}$$

Finally, by introducing the Purcell factor defined in Eq. (7) (main text), we end up with the Eqs. (10) and (11) of the main text, that is

$$\frac{\gamma_\alpha^H}{\gamma_0} = F_\alpha\left(\frac{\omega'_\alpha}{\omega_0}\right)^2\frac{\omega''^2_\alpha}{(\omega'_\alpha - \omega_0)^2 + \omega''^2_\alpha} \tag{B15}$$

$$\frac{\Delta\omega_\alpha^H}{\gamma_0} = F_\alpha\left(\frac{\omega'_\alpha}{\omega_0}\right)^2\frac{\omega''_\alpha}{2}\frac{\omega'_\alpha - \omega_0}{(\omega'_\alpha - \omega_0)^2 + \omega''^2_\alpha}\,. \tag{B16}$$

D. Derivation of Eqs. (12), (13), (15) and (16)

Here we derive the expressions of the decay rate and Lamb shift, in the single-resonance approximation, for two particular detunings of the natural QE frequency ω_0 compared to the QNM resonance frequency ω'_α: $\omega_0 = \omega'_\alpha \mp \omega''_\alpha$, for which the Lamb shift presents an extremum (indicated by arrows in Fig. 1 (b) and (d) in the main text).

We start with the detuning $\omega_0 = \omega'_\alpha + \omega''_\alpha$. By replacing ω_0 by $\omega'_\alpha + \omega''_\alpha$ in Eqs. (10) and (11), one gets

$$\frac{\gamma_\alpha^H}{\gamma_0} = \frac{1}{2}F_\alpha\left(\frac{\omega'_\alpha}{\omega'_\alpha + \omega''_\alpha}\right)^2 = \frac{1}{2}F_\alpha\left(\frac{1}{1-\frac{1}{2Q_\alpha}}\right)^2 \tag{B17}$$

$$\frac{\Delta\omega_\alpha^H}{\gamma_0} = -\frac{1}{4}F_\alpha\left(\frac{\omega'_\alpha}{\omega'_\alpha + \omega''_\alpha}\right)^2 = -\frac{1}{4}F_\alpha\left(\frac{1}{1-\frac{1}{2Q_\alpha}}\right)^2 \tag{B18}$$

where we used the fact that $Q_\alpha = -\omega'_\alpha/(2\omega''_\alpha)$. In the single-resonance approximation, Eqs. (8) and (9) thus reduce to

$$\frac{\gamma^*}{\gamma_0} = 1 + \frac{\gamma_\alpha^H}{\gamma_0} - 2\frac{\Delta\omega_\alpha^H}{\gamma_0}\frac{\mathrm{Im}(1/V_\alpha)}{\mathrm{Re}(1/V_\alpha)} \tag{B19}$$

$$\frac{\Delta\omega}{\gamma_0} = \frac{\Delta\omega_\alpha^H}{\gamma_0} + \frac{1}{2}\frac{\gamma_\alpha^H}{\gamma_0}\frac{\mathrm{Im}(1/V_\alpha)}{\mathrm{Re}(1/V_\alpha)}\,, \tag{B20}$$

and by employing the previous expressions of γ_α^H and $\Delta\omega_\alpha^H$, one gets

$$\frac{\gamma^*}{\gamma_0} = 1 + \frac{1}{2}F_\alpha\left(\frac{1}{1-\frac{1}{2Q_\alpha}}\right)^2\left[1 + \frac{\mathrm{Im}(1/V_\alpha)}{\mathrm{Re}(1/V_\alpha)}\right] \tag{B21}$$

$$\frac{\Delta\omega^-}{\gamma_0} = -\frac{1}{4}F_\alpha\left(\frac{1}{1-\frac{1}{2Q_\alpha}}\right)^2\left[1 - \frac{\mathrm{Im}(1/V_\alpha)}{\mathrm{Re}(1/V_\alpha)}\right]\,. \tag{B22}$$

Similarly, for the detuning $\omega_0 = \omega'_\alpha - \omega''_\alpha$, replacing ω_0 in Eqs. (10) and (11) yields

$$\frac{\gamma_\alpha^H}{\gamma_0} = \frac{1}{2}F_\alpha\left(\frac{\omega'_\alpha}{\omega'_\alpha - \omega''_\alpha}\right)^2 = \frac{1}{2}F_\alpha\left(\frac{1}{1+\frac{1}{2Q_\alpha}}\right)^2 \tag{B23}$$

$$\frac{\Delta\omega_\alpha^H}{\gamma_0} = \frac{1}{4}F_\alpha\left(\frac{\omega'_\alpha}{\omega'_\alpha - \omega''_\alpha}\right)^2 = \frac{1}{4}F_\alpha\left(\frac{1}{1+\frac{1}{2Q_\alpha}}\right)^2\,. \tag{B24}$$

Then, by plugging these equations in the expressions of the decay rate and Lamb shift in the single-resonance case as previously, one gets

$$\frac{\gamma^*}{\gamma_0} = 1 + \frac{1}{2}F_\alpha\left(\frac{1}{1+\frac{1}{2Q_\alpha}}\right)^2\left[1 - \frac{\mathrm{Im}(1/V_\alpha)}{\mathrm{Re}(1/V_\alpha)}\right] \tag{B25}$$

$$\frac{\Delta\omega^+}{\gamma_0} = \frac{1}{4}F_\alpha\left(\frac{1}{1+\frac{1}{2Q_\alpha}}\right)^2\left[1 + \frac{\mathrm{Im}(1/V_\alpha)}{\mathrm{Re}(1/V_\alpha)}\right]\,. \tag{B26}$$

Note that for the Hermitian systems, the decay rate and Lamb shift for these two particular detunings are given by Eqs. (B21), (B22), (B25) and (B26) with $\mathrm{Im}(1/V_\alpha) = 0$, and one ends up with the Eqs. (12) and (13) of the main text.

ACKNOWLEDGEMENTS

The authors thank Rémi Colom for fruitful discussions. E. L. would like to thank the Doctoral School "Physique et Sciences de la Matière" (ED 352) for its funding.

[1] A. F. Koenderink, ACS Photonics **4**, 710 (2017).
[2] M. Decker and I. Staude, Journal of Optics **18**, 103001 (2016).
[3] F. Marquier, C. Sauvan, and J.-J. Greffet, ACS photonics **4**, 2091 (2017).
[4] P. T. Kristensen, C. Van Vlack, and S. Hughes, Optics letters **37**, 1649 (2012).
[5] C. Sauvan, J.-P. Hugonin, I. Maksymov, and P. Lalanne, Physical Review Letters **110**, 237401 (2013).
[6] E. Muljarov and W. Langbein, Physical Review B **94**, 235438 (2016).
[7] C. Van Vlack, P. T. Kristensen, and S. Hughes, Physical Review B **85**, 075303 (2012).
[8] E. Lassalle, A. Devilez, N. Bonod, T. Durt, and B. Stout, JOSA B **34**, 1348 (2017).
[9] H. T. Dung, L. Knöll, and D.-G. Welsch, Physical Review A **62**, 053804 (2000).
[10] H. T. Dung, L. Knöll, and D.-G. Welsch, Physical Review A **64**, 013804 (2001).
[11] L. Novotny and B. Hecht, *Principles of nano-optics* (Cambridge university press, 2012).
[12] J. M. Wylie and J. E. Sipe, Phys. Rev. A **32**, 2030 (1985).
[13] C. Sauvan, J.-P. Hugonin, R. Carminati, and P. Lalanne, Physical Review A **89**, 043825 (2014).
[14] M. Doost, W. Langbein, and E. A. Muljarov, Physical Review A **90**, 013834 (2014).
[15] X. Zambrana-Puyalto and N. Bonod, Physical Review B **91**, 195422 (2015).
[16] B. Stout, A. Devilez, B. Rolly, and N. Bonod, JOSA B **28**, 1213 (2011).
[17] B. Rolly, B. Bebey, S. Bidault, B. Stout, and N. Bonod, Physical Review B **85**, 245432 (2012).
[18] A. D. Rakić, A. B. Djurišić, J. M. Elazar, and M. L. Majewski, Applied optics **37**, 5271 (1998).
[19] F. Hao and P. Nordlander, Chemical Physics Letters **446**, 115 (2007).
[20] V. Grigoriev, A. Tahri, S. Varault, B. Rolly, B. Stout, J. Wenger, and N. Bonod, Physical Review A **88**, 011803 (2013).
[21] T. Zhan and S. Chui, Physical Review A **90**, 023802 (2014).
[22] S. Ching, H. Lai, and K. Young, JOSA B **4**, 2004 (1987).
[23] V. Dodonov and A. Dodonov, Physica Scripta **90**, 074049 (2015).